Available online at http://scik.org

J. Math. Comput. Sci. 11 (2021), No. 5, 5213-5230

https://doi.org/10.28919/jmcs/5940

ISSN: 1927-5307

MAGNETO-RADIATIVE ANALYSIS OF THERMAL EFFECT IN SYMMETRICAL STENOTIC ARTERIAL BLOOD FLOW

F. H. OYELAMI[1,*], E. O. IGE[2,3], N. O. TAIYESE[2], O. Y. SAKA-BALOGUN[1]

[1]Department of Mathematical and Physical Sciences, Afe Babalola University, Ado-Ekiti, 360231, Nigeria

[2]Department of Mechanical and Mechatronics Engineering, Afe Babalola University, Ado-Ekiti, 360231, Nigeria

[3]Department of Biomedical Engineering, Afe Babalola University, Ado-Ekiti, 360231, Nigeria

Abstract: Recent reports revealed that magnetic field mediated radiotherapy is rapidly broading in the areas of soft tissue therapy. Hence, the growing concerns to provide explanations for inclusion of field-imposed radiation in critical domains of arteriosclesis. Extending the reach of previous numerical reports, the present study implemented mathematical formulations based continuum assumption. Numerical computation was executed using spectra homotopy analysis to explain field-mediated reedition of physiological fluid in the regions of arteriosclerosis. Rheology of blood was considered to follow the Casson model and the region of stenoses was treated as symmetrical constriction within the arterial microvessel. Increase in blood viscosity parameter i.e Casson number suffer decline with velocity of flow within the stenotic region. The defining thermal Grashoff parameter accelerates at the upstream flow region and decreases at the trailing edge of the physiological flow field. Further investing on radiation showed an increased projection of thermal energy while the flow field experienced viscous drag in the proximity of stenosis. Thermal stability in the presence of magnetic field reveal that drag perfusion as observed in the study could be

*Corresponding author

E-mail address: oyelamifunmilayo@abuad.edu.ng

Received April 28, 2021

harnessed to implement target delivery of radiation therapy within the region of stenosis.

Keywords: magnetic-mediated; spectra homotopy method; arterial blood; stenosed vessels; radiotherapy.

2010 AMS Subject Classification: 76Z05, 92B05.

1. INTRODUCTION

Over the years, thermal medicine has been employed as a veritable tool for therapeutic purposes on some diseases including cancer. Although growing efforts to understand and expand the capacities of thermal therapies are ongoing [1], remarkable progress in radiation physics has been a constant source of motivation to several clinical interventions and device engineering in thermal medicine [2], [3]. It has been established that the interaction between blood vessels and externally-imposed magnetic field generates magnetic torque because of the conducting cum paramagnetic properties in hemoglobin constituent in blood [4], [5]. More so, magnetic hyperthermia especially in the presence of nanoparticle-mediated thermal therapy procedures has been highly crucial in the management of tumors in cancer patients. For instance, the use of biophysical means which may include an externally imposing magnetic field could alter plaques of atherosclerotic nature without damage to arterial vessels. Essentially, the Lorentz force created due to interaction of the magnetic field on a moving conducting blood stream has the potentials to constitute viscous drag effects on the flow field, the influence of which could actuate the flow blood [6],[7]. During this interaction and its consequent pumping action, redistribution of thermal energy may lead to thermal radiation within the blood stream. Under sustained control of peripherally imposed magnetic flux, the vorticity component of the resulting drag force on the blood stream may sufficiently produce thermal radiation effect that could be significant enough to determine transport within the flow field. Thus manipulation of magnetic field based thermal radiation could be become a tool for thermal radiation therapy in clinical settings [8].

The role of thermal radiation in medicine during certain cardiac dysfunctions have been identified, a credible example is in atherosclerosis. The deposition of plagues in the cholesterol-based

biological materials on the pathways of blood vessels constitutes constrictions otherwise known as stenosis which reduces the hydraulic diameter of the flow conduit. In cases of acute stenosis, the impedance effect offered by the geometric features of stenosis on blood flow becomes evident by pressure drop which may be significant as per the severity of the stenotic barrier in the fluid conduit. The potential of this geometric development in the passage of bloodstream was earlier insight on this subject by [9] provided on baseline analysis of pressure drop emanating from modified stenotic regions in the path of blood flow. The author confirmed a nonlinear relationship between the stenosed arterial vessel and pressure drop across the region of stenosis creates which corroborated [10] and [11]. Recent studies of [12] categorically highlighted hemodynamic implications of stenosis in arterial vessels to include pressure drop by utilizing numerical schemes. Since it has been identified that stenosis impedes blood flow while the magnetic field could generate thermal radiation effect, it could suffice to examine the contribution of the magnetic field to thermal radiation in stenotic environment.

Based on its robustness and flexibility of handing, numerical investigations have been a favored tool for investigation on controlling blood circulation under the magnetic field for a varied scenario of ischemia, atherosclerosis, and related cancer ailments. Earlier experimental reports on the capacity of the magnetic field to control hemodynamics in arterial vessels notable amongst is [13] for which theoretical studies by [14] corroborated the same fact on the strength of well-posed mathematical models. Several studies supporting the same claim in the literature include [15]–[19]. Special considerations in numerical analysis on blood flow in the magnetic field environment itemized as wall behavior concerning the generation of shear stresses and velocity gradient have been sufficiently reported especially under external field influence [20],[21]. Besides, the dependence of shear stress on permeability of the conducting vessel, the interactions of wall stress on incidences of stenosis along the path of blood flow may impact the control potential of surface flux induced by magnetic field presence [22], [23].

With the inclusion of magnetic particles into the bloodstream, [24] showed that both the velocity of blood and magnetic particle could influence increasing the magnitude of the magnetic field

could yield a decline in velocity component as well as the magnetic particles embedded in blood flow. [25] Showed that in a stenotic conduit, a higher influence of magnetic field imposition was observed to results to decrease the magnitude of the velocity field in the bloodstream. The investigation of [19] described thermal radiation as a tool to addressing resistance to blood witnessed in arterial stenosis when such conduits are placed in the region of the magnetic field in a numerical experiment using a power series expansion scheme. In a recent report, [26] delineated through the use of Differential Transform Method (DTM) the impact of the magnetic field and heat radiation on flow parameters of blood in a stenosed region of an inclined arterial conduit. Treating blood flow in the stenotic region, certain assumptions about blood rheology have been presented, [27] treated blood as no-Newtonian fluid using Bingham plastic constitutive model to allow the study to explore the impact of axial velocity, yield stress and viscosity component of blood on stenosis in the blood vessel. Other reports in [28] considered blood flow in a stenotic area in coronary bypass as the Carreau-Yasuda model to account for the shear-thinning effect. [29] Examined blood flow to the power-law model to numerically examine the dependence of overlapped stenotic arteries on resistance impendence, flow rate, and wall shear stress. [30] Investigated thermal radiation in stenotic arteries under the magnetic field on the assumption of blood as a Newtonian fluid. Careful consideration of hematocrit variation was also reported using first partial derivative with second-order central difference scheme.

In this paper, we examine thermal radiation effect on blood flow in the symmetrically stenotic arterial vessel in a magnetic field environment. The magnetically conducting blood is treated to follow the Casson constitutive model and generalized differential approximation of radiative heat was assumed following [31]. Stenotic obstructions in the blood vessel are captured via a constriction model following bell-shaped geometric representation. The study is intended to provide insights into magnetic field effects on circulating of blood flow which has been treated with much attention over the years largely because of its potentials to inspired clinical procedure and technologies around heart-related illnesses.

2. MATHEMATICAL FORMULATION

Consider an incompressible non-Newtonian casson fluid through a stenotic artery. The gravitational field is considered dominant in the reverse direction to x-axis. The viscosity of the blood in the stenotic artery is considered to vary in this study because there is too much accumulation of red blood cells in the arterial center line. It was assumed that the temperature of blood and that of the artery is high such that radiative heat transfer can take place. Magnetic field is transversely applied in a perpendicular direction to the flow filed. The assumption made that both electromagnetic force and electrical conductivity is sufficiently small. The Boussinesq approximation is valid.

According to fluid viscosity definition ($\tau=\mu\frac{dU}{dy}\Big|_y=0$), the Casson model employed to describe blood deformation in the presence of field force is described in [32];

$\tau_{i,j}= (\mu_b + \frac{p_y}{\sqrt{2\Pi}})\ 2e_{ij}$ when $\pi > \pi_c$ (1)

$\tau_{i,j}= (\mu_b + \frac{p_y}{\sqrt{2}\pi_c})\ 2e_{ij}$ when $\pi < \pi_c$ (2)

P_y is the yield stress of the fluid given as

$$P_y = \frac{\mu_b\sqrt{2\Pi}}{\beta} \quad (3)$$

Where μ_b is the plastic dynamic viscosity, $\Pi = e_{i,j}.e_{i,j}$ is the resultant component describing rate of deformation of the biogenic transport fluid and e_{ij} represent the measure of deformation and π_c is the determining estimate that depends on Casson parameter. Consider y $\pi > \pi_c$, we can have that;

$$\mu_o = \mu_b + \frac{P_y}{\sqrt{2\Pi}} \quad (4)$$

Substituting equation 4 into 3 to obtain that the kinematic viscosity depending on the plastic dynamic viscosityμ_b, density ρ, Casson parameter β yields

$$\mu_o = = \frac{\mu_b}{\rho}\left(1 + \frac{1}{\beta}\right) \quad (5)$$

Considering the assumptions above and the rheological equations of the Casson model, the governing equation becomes

$$-\frac{\partial \bar{p}}{\partial \bar{x}}+\frac{1}{r}\left(1+\frac{1}{\beta}\right)\frac{\partial}{\partial r}\left(r\mu\frac{\partial u}{\partial r}\right)-\sigma_e\beta_o^2u+g\rho\beta(T-T_o)=0 \quad (6)$$

$$k\frac{1}{r}\frac{\partial}{\partial r}\left(r\frac{\partial T}{\partial r}\right)-\frac{\partial q_r}{\partial r}+Q_o(T-T_o)=0 \quad (7)$$

Subjected to the boundary conditions

$$\frac{\partial u}{\partial r}=\frac{\partial T}{\partial r}=0 \quad \text{at } r=0 \quad (8)$$

$$u=0,\ T=T_w \quad \text{at } r=R(x) \quad (9)$$

the variable u represent the horizontal velocity component, T is temperature of blood, T_w is the temperature at the wall of arterial vessel, T_o is the characteristic temperature of blood as the biogenic fluid, g accounts for gravity parameter, ρ density of blood, β coefficient of thermal expansion, B_o magnetization intensity, σ_e is the blood electric conductivity, K thermal conductivity of the blood and p captures pressure estimate of blood. The stenosis geometry is given by

$$\frac{R(\bar{x})}{R_o}=\delta(\bar{x})=1-\frac{\delta}{R_o}\exp\left(-\frac{\lambda^2\varepsilon^2\bar{x}^2}{R_o^2}\right) \quad (10)$$

$R(\bar{x})$ represent blood vessel radius within stenosis constriction, R_o reference radius of blood vessel, δ stenosis pitch section of contraction, λ parameter constant, ε is used to characterize the baseline length of the constriction. The differential model that captures relative heat flux within the region of stenosis as contained in [31] and defined in this study as

$$\frac{\partial}{\partial r}\left(\frac{1}{\alpha}\frac{\partial q_r}{\partial r}\right)-3\alpha^2q_r-16\sigma\alpha T^3\frac{\partial T}{\partial r}=0 \quad (11)$$

Where α defines the absorption coefficient while σ Steffan-Boltzman constant. This study considers an optically thin fluid such that $\alpha << 1$, hence the radiative heat flux becomes

$$\frac{\partial q_r}{\partial r}=4\alpha\sigma(T_o^4-T^4) \quad (12)$$

The study follows [33] to express the cross-sectional fluctuation in the viscosity of blood μ(r) given by:

$$\mu(r)=\mu_o\,[1+ch(r)] \quad (13)$$

where c is a constant and it is considered in this study to be 3 while $h(r)$ is the hematocrit

expression defined by [19] is here stated:

$$h(r) = h_m\left[1 - \left(\frac{r}{R_0}\right)n\right] \tag{14}$$

where h_m is the critical hematocrit within the blood vessel and m represents the real number defined by the criterion $m \geq 2$. The value of n determines the profile shape. The following quantities are introduced on the governing equations in this study.

$$\text{y}=\frac{r}{R_o},\ w = \frac{u}{U},\ \theta = \frac{T-T_o}{T_w-T_o},\ \text{Gr} = \frac{g\rho\beta(T_w-T_o)R_0^2}{U\mu_o}$$

$$\text{M} = \frac{\sigma_e\beta_0^2R_0^2}{\mu_o},\ a_1 = \frac{\delta}{R_o},\ \text{R}_\text{a} = \frac{4\sigma\alpha R_0^2(T_w-T_o)}{K},\ \text{a} = 1+ch_m \tag{15}$$

$$\text{b} = ch_m,\quad x = \frac{\bar{x}}{R_o},\ \text{P} = \frac{\bar{P}R_o}{U\mu_o},\ \text{L} = -\frac{d\bar{P}}{dx},\ a_2 = \varepsilon^2\lambda^2, r = \frac{T_0}{T_w-T_0}$$

Using equations 12, 13, 14 and 15 in equations 6 and 7, we obtain the following dimensionless equation

$$L + \frac{1}{y}\frac{\partial}{\partial y}\left[y(a-by^n)\frac{\partial w}{\partial y}\right] - Mw + Gr\theta = 0 \tag{16}$$

$$\frac{1}{y}\frac{\partial}{\partial y}\left(y\frac{\partial\theta}{\partial y}\right) + R_a[(\theta+r)^4 - r^4] = 0 \tag{17}$$

The physical quantity of importance to hemodynamic study are: skin friction(S_f), Nusselt number (Nu). They are computed in this study as follows:

Skin friction $\left(S_f\right) = \frac{\tau_w}{\rho U_w^2}$

where $\tau_w = \mu\left(1+\frac{1}{\beta}\right)\left(\frac{\partial u}{\partial r}\right)_{r=0}$

Also, Nusselt number $(Nu) = \frac{xq_w}{\alpha(T_w-T_o)}$

Where the rate of heat transfer q_w is given as

$$q_w = -\alpha\left(\frac{\partial T}{\partial r}\right)_{r=0}$$

The computational values of different parameters on the above physical quantities of engineering interest are computed in table 1.

3. METHOD OF APPROACH

The numerical technique implemented in this study is a modification of Homotopy Analysis

Method described as Spectra Homotopy Analysis Method (SHAM) which was utilized as presented in [34]. SHAM is based on a combined methods of HAM and Chebyshev variant of spectra collocation. The process of applying SHAM entails the transformation from $[0,\infty)$ to [-1,1] with required truncation. For this study, Chebyshev spectra was employed following the mapping function given as:

$$\xi = \frac{2\eta}{L} - 1, \qquad \xi \in [-1, 1] \tag{18}$$

The homogenous boundary condition is applied on SHAM given as:

$$w(\eta) = w(\xi) + w_o(\eta), \qquad w_o(\eta) = 1 - e^{-\eta} \tag{19}$$

$$\theta(\eta) = \theta(\xi) + \theta_o(\eta), \qquad \theta_o(\eta) = e^{-\eta} \tag{20}$$

where $w_o(\eta)$ and $\theta_o(\eta)$ contains initial assumption follows $w(\eta)$ and $\theta(\eta)$ respectively. Substituting equations (19) and (20) into the transformed governing equations 16 and 17 gives

$$L + a\left(1+\frac{1}{\beta}\right)w'' + \frac{a}{y}\left(1+\frac{1}{\beta}\right)w' - by^n\left(1+\frac{1}{\beta}\right)w'' + y^n(1+\eta)w' - Mw + Gr\theta = -a\left(1+\frac{1}{\beta}\right)w_o'' - \frac{a}{y}\left(1+\frac{1}{\beta}\right)w_o' + by^n\left(1+\frac{1}{\beta}\right)w_o'' - y^n(1+n)w_o' + Mw_o - Gr\theta_o \tag{21}$$

$$\theta'' + \frac{1}{y}\theta' + Ra\theta^4 + 4Ra\theta_o\theta^3 + 6Ra\theta_o^2\theta^2 + 4Ra\theta_o^3\theta + 4Rar\theta^3 + 12Rar\theta_o\theta^2 + 12Rar\theta_0^2\theta + 6Rar^2\theta^2 + 12Rar^2\theta_o\theta + 4Rar^3\theta = -\theta_o'' - \frac{1}{y}\theta_o' - Ra\theta_o^4 - 4Rar\theta_o^3 - 6Rar^2\theta_o^2 - 4Rar^3\theta_o \tag{22}$$

Setting; $a_1 = a\left(1+\frac{1}{\beta}\right)$, $a_2 = \frac{a}{y}\left(1+\frac{1}{\beta}\right)$, $a_3 = -by^n\left(1+\frac{1}{\beta}\right)$, $a_4 = y^n(1+n)$

$b_1 = \frac{1}{y}$, $b_2 = 4Ra\theta_o$, $b_3 = 6\,Ra\theta_o^2$, $b_4 = 4Ra\theta_o^3$, $b_5 = 12Rar\theta_o$, $b_6 = 12\,Rar\theta_o^2$

$b_7 = 6Rar^2$, $b_8 = 12Rar^2\theta_o$, $b_9 = 4Rar^3$

$$H_1(\eta) = -a\left(1+\frac{1}{\beta}\right)w_0'' - \frac{a}{y}\left(1+\frac{1}{\beta}\right)w_o' + by^n\left(1+\frac{1}{y}\right)w_o' - y^n(1+n)w_o' + Mw_o - Gr\theta_o + L$$

$$H_2(\eta) = -\theta_0'' - \frac{1}{y}\theta_o' - Ra\theta_o^4 - 4Rar\theta_o^3 - 6Rar^2\theta_o^2 - 4Rar^3\theta_o$$

Substituting the above coefficient parameters into equations (21) and (22) to obtain;

$$L + a_1w'' + a_2w' + a_3w'' + a_4w' - Mw + Gr\theta = H_1(\eta) \tag{23}$$

$$f\quad \theta'' + b_1\theta' + Ra\theta^4 + b_2\theta^3 + b_3\theta^2 + b_4\theta + 4Rar\theta^3 + b_5\theta^2 + b_6\theta + b_7\theta^2 + b_8\theta + b_9\theta =$$

$H_2(\eta)$ (24)

Chebyshev pseudo-spectral method (CPM) is applied to solve equations (23) and (24) and all unknown functions such as w(ξ) and θ(ξ) are estimated and terminated series of Chebyshev polynomic defined as;

$w(\xi) = \sum_{k=0}^{N} w_k T_k\ (\varepsilon_j)$, $\theta(\xi) = \sum_{k=0}^{N} \theta_k T_k\ (\varepsilon_j)$ (25)

where $\varepsilon_o, \varepsilon_1, \varepsilon_2, \ldots\ldots, \varepsilon_n$ are Gauss Lobatto collocation points contained in [35] implemented as defined by [36] as

$\varepsilon_j = \cos\frac{\pi_j}{N}$, j = 0,1,2,….,N (26)

Where T_k represents the K^{th} Chebyshev polynomial, collocation number point defined as N+1 is the number of collocation points. The derivatives of the unknown functions w(ξ) and θ(ξ) at the collocation points are given as:

$\frac{d^r w}{d\eta^r} = \sum_{K=0}^{N} \overline{D}_{kj} w(\varepsilon)$, $\frac{d^r \theta}{d\eta^r} = \sum_{k=0}^{N} \overline{D}_{kj}^{r} \theta(\varepsilon)$ (27)

Where r is the order of the differentiation and $\overline{D} = \frac{2}{L}\overline{D}$ [37] and $\overline{D}$ is the chebyshev spectral differentiation matrix. Now substituting equations (25) and (27) into (23) and (24) to obtain the following form of matrix

$$\begin{bmatrix} A_{11} & A_{12} \\ A_{21} & A_{22} \end{bmatrix} \begin{bmatrix} w \\ \theta \end{bmatrix} = \begin{bmatrix} H_1(\eta) \\ H_2(\eta) \end{bmatrix} \quad (28)$$

The above matrices can be written in the form

$$A\varphi_L = G \quad (29)$$

Subject to;

$w_L(\varepsilon_N) = 0$, $\sum_{k=0}^{N} D_{Nk}\, w_L(\varepsilon_k) = 0$, $\sum_{K=0}^{N} D_k\, \theta_L(\varepsilon_k) = 0$ (30)

$\theta_L(\varepsilon_N) = 0$, $\theta_L(\varepsilon_o) = 0$ (31)

Where

$\varphi_L = [w_L(\varepsilon_o), w_L(\varepsilon_1), \ldots\ldots w_L(\varepsilon_N), \theta_L(\varepsilon_O), \theta_L(\varepsilon_1), \ldots.. \theta_L(\varepsilon_N)]^T$

$G = [\varphi_1(\eta_o), \varphi_1(\eta_1), \ldots\ldots \varphi_1(\eta_N), \varphi_2(\eta_o), \varphi_2(\eta_1), \ldots\ldots, \varphi_2(\eta_N)]^T$

$$A = \begin{bmatrix} A_{11} & A_{12} \\ A_{21} & A_{22} \end{bmatrix} \quad (32)$$

and

$A_{11} = a_1D^2 + a_2D + a_3D^2 + a_4D - M$

$A_{12} = Gr$, $A_{21} = 0$, $A_{22} = D^2 + b_1D + b_4 + b_6 + b_8 + b_9$

The SHAM method requires that the equations are divided into components of linear and nonlinear terms. The linear parts operators of the problem at study is given as;

$$a_1w'' + a_2w' + a_3w'' + a_4w' - Mw + Gr\theta + L = H_1(\eta) \quad (32)$$

$$\theta'' + b_1\theta' + b_4\theta + b_6\theta + b_8\theta + b_9\theta = H_2(\eta) \quad (33)$$

While the nonlinear operators are

$$Ra\theta^4 + b_2\theta^3 + b_3\theta^2 + 4Rar\theta^3 + b_5\theta^2 + b_6\theta + b_7\theta^2 = H_2(\eta) \quad (34)$$

The zeroth-order of deformation is described by the equations below

$$(1-q)L_w[w(\eta,q) - w_0(\eta)] = q\hbar_w\varphi_w(\eta)N[w(\eta,q),\theta(\eta,q)] \quad (35)$$

$$(1-q)L_\theta[\theta(\eta,q) - \theta_0(\eta)] = q\hbar_\theta\varphi_\theta(\eta)N[w(\eta,q),\theta(\eta,q)] \quad (36)$$

Where $q \ni [0,1]$ is an embedded component, $\hbar_w$, φ_w are non-zero peripherial parameters and $w(\eta,q), \theta(\eta,q)$ are unknown functions dependent on subject to the boundary conditions 30 and 31. Setting $q = 1$ in equations 35 and 36, we obtain

$$0 = q\hbar_w\varphi_w(\eta)N[w(\eta,q),\theta(\eta,q)] \quad (37)$$

$$0 = q\hbar_\theta\varphi_\theta(\eta)N[w(\eta,q),\theta(\eta,q)] \quad (38)$$

It is noted that the momentum equation does not have nonlinear terms. SHAM convergences depends on the selection of the auxiliary constant($\hbar$). This parameter decides the convergence of SHAM series solution. The estimate of $\hbar$ is selected in translational segment of $\hbar$ curve. During the implementation of the present problem, it is observed that an increased estimate of $\hbar$ yields a instantaneous results. Therefore, the default values used in the present study are $\hbar = -1.0, L = between\ 5\ and\ 12, N = 100$

4. RESULTS AND DISCUSSION

The results of thermal analysis of blood flow through an arterial stenosis in the region of magnetic field. The physics of blood flow is governed by Casson model is discussed in the light to radiation

effect due to sustained magnetic field exposure within the region of arterial stenosis.

Table 1: Numerical data for selected condition of Skin friction (Sf) and Nusselt number (Nu) parameters.

β	M	Gr	Ra	Sf	Nu
0.1	1.0	2.0	0.5	1.43656098	0.36524531
0.5	1.0	2.0	0.5	1.43768832	0.39180260
1.0	1.0	2.0	0.5	1.43902918	0.40190311
0.3	0.5	2.0	0.5	1.39780630	0.46617254
0.3	1.0	2.0	0.5	1.37516023	0.46329207
	2.0	2.0	0.5	1.35255488	0.46329207
	1.0	0.0	0.5	1.42040653	0.46904267
		0.5	0.5	1.42031963	0.66903883
		1.0	0.5	1.42023273	0.46903500
		2.0	0.1	1.43693509	0.19146116
			0.3	1.43784111	0.08245101
			0.5	1.43968272	0.07236111

Table 1 shows that higher casson parameter β increases the duo parameters of Nusselt and near arterial wall skin friction for specified Casson parameter yields increased impact of the rate of heat transport within the momentum and temperature boundary layer thickness. The imposed M-parameter on the blood flow field is presented in Table 1 to decrease the skin friction but increase the heat transfer rate. The declination on the coefficient of skin friction is because of the Lorentez force which is produced by the magnetic field strength. Also, the thermal Grashof number Gr decreases both skin friction coefficient and Nusselt number while the radiation parameter Ra enhances the fluid thermal condition by enhancing the wall-skin friction and Nusselt number.

Table 2: Computational data of Magnetic parameter of shear stress on arterial wall and thermal field

M	$-w^1(0)$	$-\theta^1(0)$
0.1	1.4578	0.8605
0.5	1.4481	0.5074
0.9	1.4392	0.8055

It is observed from table 2 that higher magnitude of magnetic flux causes decline in both wall-skin friction and thermal field.

Table 3: Computational data of Casson parameter on of shear stress on arterial wall and thermal field

B	$-w^1(0)$	$-\theta^1(0)$
0.0	2.7970	0.4359
0.5	2.8331	0.4337
1.0	2.9394	0.4272
1.5	3.1107	0.4174

Table 3 shows the computation of β on **of** shear stress on arterial wall and thermal field. Increase in β is noticed to increase shear stress on arterial wall but causes retardation in the rate of radiative temperature transport

Table 4: Computational data of Grashof parameter on shear stress at arterial wall and thermal field

Gr	$-w^1(0)$	-θ(0)
0.0	5.4873	0.6475
0.5	5.4876	0.6455
1.0	5.4879	0.6435
1.5	5.4881	0.6420

From Table 4, it is observe that Increase in the Grashof parameter yields increase on shear stress at the arterial wall and the behavior of temperature distribution.

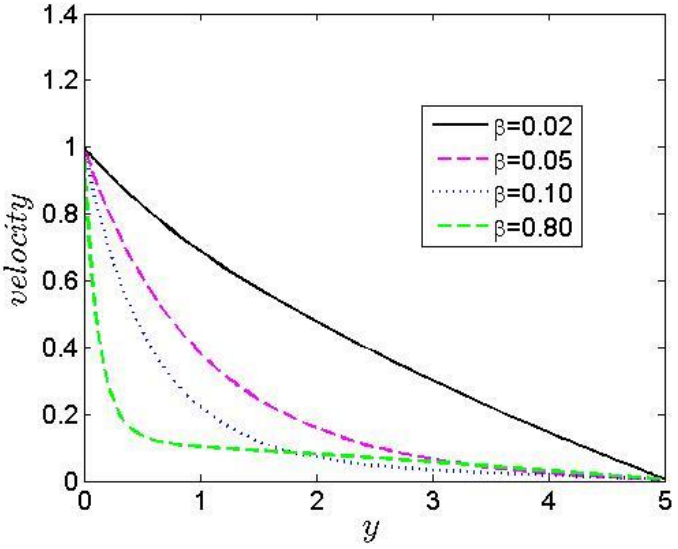

Figure 1: Influence of Casson parameter on velocity distribution.

In figure 1, increase in the value of the Casson parameter is seen to decrease the entire hydrodynamic boundary layer by decreasing the velocity distribution. Graphical observations showed that as $\beta \to \infty$ the model seems to be Newtonian by behaving like the linear behavior of Newtonian fluid which obeys the Newton's law of viscosity. The result in figure 1 means that increase in β decreases the dynamic plastic viscosity which is capable of reducing the fluid velocity.

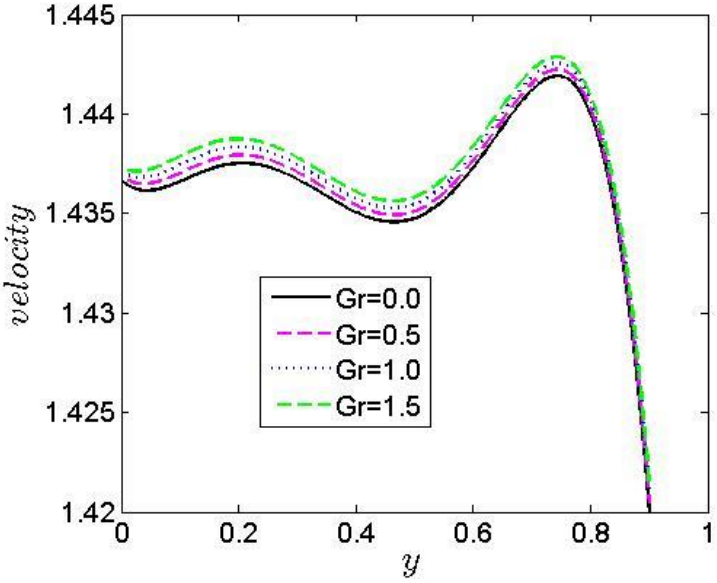

Figure 2: Infleunce of Grashof parameter on the velocity distribution

Figure 2 depicts the dominance of Grashof parameter on the distribution of velocity field. It is shown in the figure that increase in Gr accelerates the velocity profile and later decelerates. The

layer of acceleration is due to the contribution of buoyancy which is capable of bringing more intensity on the velocity of the fluid. In the absence of the buoyancy force, the profile decelerates.

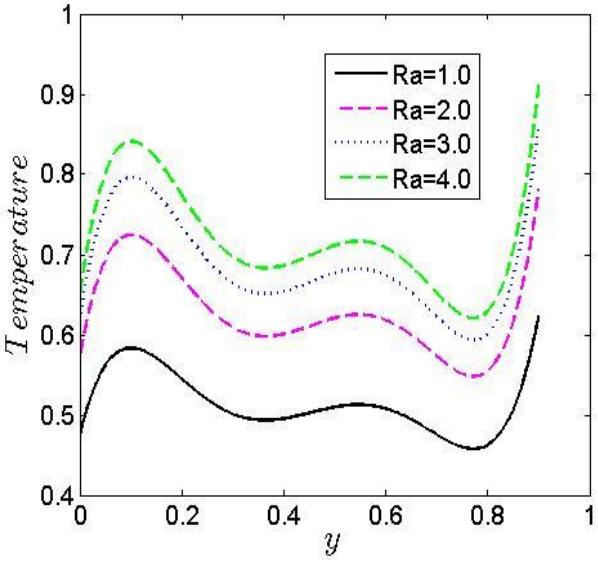

Figure 3: Influence of thermal radiation on the thermal transport

The observation of radiation effect is presented in Figure 3, graphical distribution yield increase in the rate of heat transfer. Increasing Ra led to huge thermal load in the Casson-blood fluid in in the vicinity stenosis of arterial wall. Hence, radiation quantity significantly determines the enhancement of convective transport of Casson-blood fluid and consequently accelerate the extent of temperature distribution.

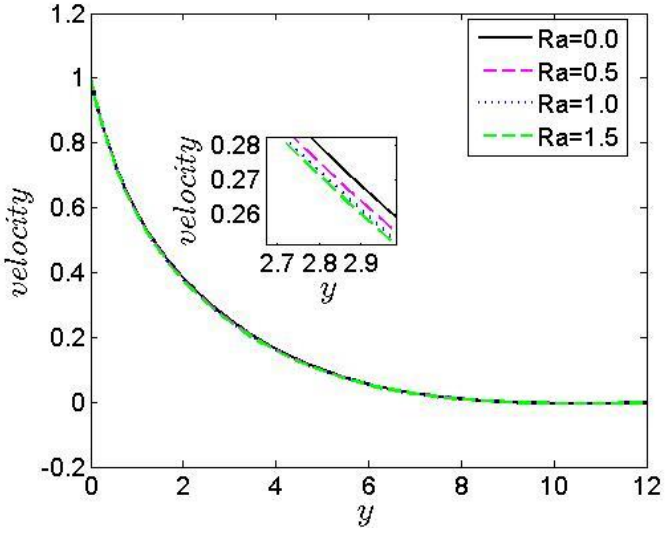

Figure 4: Influence of thermal radiation on momentum transport

Interestingly, the radiation quantity retards momentum transport of the Casson-blood fluid in the region of stenosis. Increasing Ra will reduce the fluid content that is, blood which is considered as a case study in the present work, will dry off as Ra increases.

5. CONCLUSION

- Increase in β decreases the dynamic plastic viscosity which is capable of reducing the fluid velocity.
- Radiation parameter Ra decreases the velocity profile. Increasing Ra will reduce the fluid content that is, blood which is considered as a case study in the present work, will dry off as Ra increases.
- Increase in Gr accelerates the velocity profile and later decelerates.
- Increase in the Casson-blood quantity β intensify the arterial wall-skin friction and Nusselt number i.e casson parameter has great impact on the rate of heat distribution within the momentum and thermal boundary layers.
- Magnetic M-parameter on the Casson-blood is responsible for decline in arterial wall- skin friction while intensifying distribution of thermal load as the fluid approaches the region of stenosis.
- Thermal Grashof number Gr decreases both arterial wall-skin friction coefficient and Nusselt parameter.
- Radiation parameter Ra enhances the fluid thermal condition by enhancing the arterial wall-skin friction as well as Nusselt parameter.
- Higher trend of Magnetic field parameter β is noticed to increase arterial wall shear stress but causes retardation in the rate thermal distribution in the temperature boundary layer.
- Increase in the magnetic parameter M reduces the wall shear stress and the wall heat transfer rate.
- Increase in Gr is seen to increase shear stress at the arterial wall as well as temperature distribution within the constrictions of stenosis.

CONFLICT OF INTERESTS

The author(s) declare that there is no conflict of interests.

REFERENCES

[1] A. Andreozzi, L. Brunese, M. Iasiello, C. Tucci, G.P. Vanoli, Modeling heat transfer in tumors: a review of thermal therapies, Ann. Biomed. Eng. 47 (2019), 676–693.

[2] X. Liu, L. Wang, Z.M. Zhang, Near-field thermal radiation: recent progress and outlook, Nanoscale Microscale Thermophys. Eng. 19 (2015), 98–126.

[3] S. R. Tsai, M.R. Hamblin, Biological effects and medical applications of infrared radiation, J. Photochem. Photobiol. B: Biol. 170 (2017), 197–207.

[4] L. Pauling, C. D. Coryell, The magnetic properties and structure of hemoglobin, oxyhemoglobin and carbonmonoxyhemoglobin, Proc. Natl. Acad. Sci. USA. 22 (1936), 210–216.

[5] K. L. Bren, R. Eisenberg, H. B. Gray, Discovery of the magnetic behavior of hemoglobin: A beginning of bioinorganic chemistry, Proc. Natl. Acad. Sci. USA. 112 (2015), 13123–13127.

[6] A. Thess, E. V. Votyakov, Y. Kolesnikov, Lorentz Force Velocimetry, Phys. Rev. Lett. 96 (2006), 164501.

[7] M. Liebl et al., Noninvasive monitoring of blood flow using a single magnetic microsphere, Sci. Rep. 9 (2019), 5014.

[8] S. Siddiqa, S. B. Naqvi, N. Begum, S. E. Awan, and M. A. Hossain, Thermal radiation therapy of biomagnetic fluid flow in the presence of localized magnetic field, Int. J. Therm. Sci. 132, (2018), 457–465.

[9] D. F. Young, N. R. Cholvin, and A. C. Roth, Pressure drop across artificially induced stenoses in the femoral arteries of dogs, Circ. Res. 36 (1975), 735–743.

[10] A. G. May, J. A. Deweese, and C. G. Rob, Hemodynamic effects of arterial stenosis, Surgery, 6, (1963), 395–410.

[11] S. R. Dodds, The haemodynamics of asymmetric stenoses, Eur. J. Vasc. Endovasc. Surg. 24 (2002), 332–337.

[12] Z. Malota, J. Glowacki, W. Sadowski, and M. Kostur, Numerical analysis of the impact of flow rate, heart rate, vessel geometry, and degree of stenosis on coronary hemodynamic indices, BMC Cardiovasc. Disord. 18 (2018), 132.

[13] E. M. Korchevskii and L. S. Marochnik, Magnetohydrodynamic version of movement of blood, Biophysics, (1965), 411–414.

[14] V. A. Vardanyan, Effect of a magnetic field on blood flow, Biophysics (Oxf). 18 (1973), 515–521.

[15] J. C. Misra, B. Pal, A. Pal, and A. S. Gupta, Oscillatory entry flow in a plane channel with pulsating walls, Int. J. Non. Linear. Mech. 36 (2001), 731–741.

[16] J. C. Misra, B. Pal, and A. S. Gupta, Hydromagnetic flow of a second-grade fluid in a channel - Some applications to physiological systems, Math. Model. Methods Appl. Sci. 8 (1998), 1323–1342.

[17] S. Akar, J. A. Esfahani, and S. A. Mousavi Shaegh, A numerical investigation of magnetic field effect on blood flow as biomagnetic fluid in a bend vessel, J. Magn. Magn. Mater. 482 (2019), 336–349.

[18] J. C. Misra and A. Sinha, Effect of thermal radiation on MHD flow of blood and heat transfer in a permeable capillary in stretching motion, Heat Mass Transf. und Stoffuebertragung, 49 (2013), 617–623.

[19] J. Prakash and O. D. Makinde, Radiative heat transfer to blood flow through a stenotic artery in the presence of magnetic field, Lat. Am. Appl. Res. 41 (2011), 273–277

[20] S. S. Dhawan et al., Shear stress and plaque development, Expert Review of Cardiovascular Therapy, 8 (2010), 545–556.

[21] G. Liu et al., Numerical simulation of flow in curved coronary arteries with progressive amounts of stenosis using fluid-structure interaction modelling, J. Med. Imaging Heal. Inform. 4 (2014), 605–611.

[22] N. Srivastava, Analysis of flow characteristics of the blood flowing through an inclined tapered porous artery with mild stenosis under the influence of an inclined magnetic field, J. Biophys. 2014 (2014), 797142.

[23] A. Sankar-Ramkarran, S. R. Gunakala, and D. Comissiong, Magnetohydrodynamic Stenosed Blood Flow Through Microcirculation with Permeable Walls, Int. J. Appl. Comput. Math. 4 (2018), 17.

[24] B. K. Sharma, M. Sharma, R. K. Gaur, and A. Mishra, Mathematical modeling of magneto pulsatile blood flow through a porous medium with a heat source, Int. J. Appl. Mech. Eng. 20 (2015), 385–396.

[25] G. C. Shit and M. Roy, Effect Of Induced Magnetic Field On Blood Flow Through A Constricted Channel: An Analytical Approach, J. Mech. Med. Biol. 16 (2016), 1650030–1650049.

[26] J. U. Abubakar and A. D. Adeoye, Effects of radiative heat and magnetic field on blood flow in an inclined tapered stenosed porous artery, J. Taibah Univ. Sci. 14 (2020), 77–86.

[27] O. Prakash, O. D. Makinde, S. P. Singh, N. Jain, and D. Kumar, Effects of stenoses on non-Newtonian flow of blood in blood vessels, Int. J. Biomath. 8 (2015), 15500102.

[28] J. Chen, X. Y. Lu, and W. Wang, Non-Newtonian effects of blood flow on hemodynamics in distal vascular graft anastomoses, J. Biomech. 39 (2006), 1983–1995.

[29] Z. Ismail, I. Abdullah, N. Mustapha, and N. Amin, A power-law model of blood flow through a tapered overlapping stenosed artery, Appl. Math. Comput. 195 (2008), 669–680.

[30] T. Chinyoka and O. D. Makinde, Computational dynamics of arterial blood flow in the presence of magnetic field and thermal radiation therapy, Adv. Math. Phys. 2014 (2014), 915460.

[31] P. Cheng, Two-dimensional radiating gas flow by a moment method, AIAA J. 2 (1964), 1662–1664.

[32] S. Pramanik, Casson fluid flow and heat transfer past an exponentially porous stretching surface in presence of thermal radiation, Ain Shams Eng. J. 5 (2014), 205–212.

[33] E. W. Merrill, E. R. Gilliland, G. Cokelet, H. Shin, A. Britten, and R. E. Wells, Rheology of blood and flow in the microcirculation, J. Appl. Physiol. 18 (1963), 255–260.

[34] S. S. Motsa, P. Sibanda, and S. Shateyi, A new spectral-homotopy analysis method for solving a nonlinear second order BVP, Commun. Nonlinear Sci. Numer. Simul. 15 (2010), 2293–2302.

[35] C. Canuto, M. Y. Hussaini, A. Quarteroni, and T. A. Zang, Spectral Methods in Fluid Dynamics, Springer, 1988.

[36] A. I. Fagbade, B. O. Falodun, and A. J. Omowaye, MHD natural convection flow of viscoelastic fluid over an accelerating permeable surface with thermal radiation and heat source or sink: Spectral Homotopy Analysis Approach, Ain Shams Eng. J. 9 (2018), 1029–1041

[37] L. N. Trefnethe, Spectral Methods in MATLAB, SIAM, 2000.